MECOM99
Mendoza
6-10 de septiembre de 1999

TIME-DOMAIN SIMULATIONS OF NONLINEAR, UNSTEADY, AEROELASTIC BEHAVIOR

Sergio Preidikman[a] and Dean T. Mook[b]

[a]Facultad de Ingeniería
Universidad Nacional de Río Cuarto
Ruta Nacional 36 Km 601
(5800) Río Cuarto, Provincia de Córdoba, Argentina

[b]Department of Engineering Science and Mechanics
Virginia Polytechnic Institute and State University
Blacksburg, VA 24061-0219, USA

RESUMEN

Se describe un método para simular el comportamiento aeroelástico inestacionario, no lineal, y subsónico de un ala de avión. El flujo del aire y la estructura del ala son considerados elementos de un único sistema dinámico. Las ecuaciones governantes son integradas numéricamente, simultáneamente e interactívamente, en el dominio del tiempo. Para predecir las cargas aerodinámicas se utiliza nuestra versión del método general de red de vórtices discretos (Vortex-Lattice Method). Para modelar la estructura se utiliza un modelo de elementos finitos lineal; el mismo fue generado mediante MSC/NASTRAN. Los dos modelos antes citados son combinados de forma tal que las mallas estructurales y aerodinémicas pueden ser elegidas arbitrariamente. El campo de deformaciones del ala se expresa como una combinación lineal de sus modos de vibrar libremente, los que son obtenidos del modelo de elementos finitos, y los coeficientes de esta combinación lineal son considerados como las coordenadas generalizadas del sistema dinámico. Un método predictor-corrector es adaptado para obtener la historia en el tiempo de las coordenadas generalizadas y del flujo de aire. Los resulatos numéricos muestran claramente que, cuando la velocidad es baja, la respuesta a condiciones iniciales no triviales decae y contiene más de una frecuencia. Sin embargo al aumentar la velocidad y/o el ángulo de ataque, el movimiento comienza a organizarse (la energía se concentra alrededor de muy pocas frecuencias). Finalmente, cuando se llega a la velocidad de "Flutter" (la velocidad crítica), todos los modos, después de un transitorio, responden a la misma frecuencia. Las simulaciones indican que el factor causante de "Flutter" es un bifurcacién de Hopf supercrítica. A velocidades mayores que la crítica, la amplitud de las respuestas parece, inicialmente, crecer linealmente con el tiempo, luego se transforman en ciclos límites. La amplidud de estos ciclos límites aumenta a medida que la velocidad aumenta, y eventualmente sufren una segunda bifurcación de Hopf supercrítica y se vuelven inestables; sus amplitudes y fases son moduladas. En este punto la respuesta puede ser descripta como el movimiento en un toro.

ABSTRACT

A method for simulating unsteady, nonlinear, subsonic aeroelastic behavior of an aircraft wing is described. The flowing air and deforming structure are treated as the elements of a single dynamic system, and all of the governing equations are integrated numerically, simultaneously, and interactively in the time domain. Our version of the general nonlinear, unsteady, vortex-lattice method is used to predict the aerodynamic forces, a linear finite-element model of the wing, which is derived from MSC/NASTRAN, is used to predict the deformations of the wing, and the models are coupled in such a way that the structural and aerodynamic grids can be chosen arbitrarily. The deformation of the wing is expressed as an expansion in terms of the linear free-vibration modes obtained from the finite-element model, and the time-dependent coefficients in the expansion serve as the generalized coordinates for the entire dynamic system. A predictor-corrector method is adapted to solve for the generalized coordinates and the flowfield. The results clearly show that, when the speed is low, the responses to initial disturbances contain many frequencies and decay, but that the responses become more organized (energy concentrates around a few frequencies) as the speed and/or the angle of attack increases. Finally, at the onset of flutter, all of the modes, after an initial transient period, respond at the same frequency. It appears that the flutter-causing instability is a supercritical Hopf bifurcation. At and above the critical speed, the amplitudes of the responses appear to grow linearly with time initially, but then become limit

cycles. The amplitudes of the limit cycles grow as the speed increases, and eventually it appears that the limit cycles experience a secondary supercritical Hopf bifurcation and become unstable; their amplitudes and phases modulate. At this point the response can be described as motion on a torus.

INTRODUCTION

In this article, we present a method to simulate unsteady, nonlinear, subsonic (more precisely, incompressible), aeroelastic behavior, and to demonstrate the method we focus on wing flutter. Our approach is to treat the flowing air and the wing structure as elements of a single dynamic system and to numerically integrate all of the governing equations simultaneously and interactively in the time domain. In so doing, we calculate the flowfield and the motion of the wing simultaneously. We did not want to restrict the present simulation to linear equations of motion or periodic responses; hence, the classical approaches to resolving this dilemma were not applicable here. The present simulation is not restricted to periodic motions or linear governing equations; as a result, it can predict sub- and super-critical behavior and is a very effective tool for designing control systems to suppress flutter and reduce gust response.

The development of the current simulation required the development of four essential components: (1) an aerodynamic model to predict the loads on the wing, (2) a structural model to predict the response of the wing to these loads and to provide the boundary conditions for the flowfield, (3) a method to combine the two models, and (4) a method to integrate all of the governing equations simultaneously and interactively. These are briefly discussed in the following: then some results are presented, and finally there are some brief concluding remarks.

It would be impossible to review all the literature related to flutter. But, suffice it to say that the present work is part of a new approach that is currently receiving considerable attention in a number of different places. It extends the work of Strganac and Mook[1] and Luton and Mook.[2] It is not the first to use the concepts underlying the general unsteady vortex-lattice method, but it does add some innovations to the procedure. It is not the first to use a finite-element model of the wing, but, as far as we know, it is the first to combine the general, nonlinear, unsteady vortex-lattice method with an industry-standard, finite-element method. The result is a simulation in the time domain that clearly reveals the physics of flutter among other phenomena.

In the work that, perhaps, is most closely related to the present work, Tang *et al.*[3] recently found limit-cycle oscillations by using nonlinear plate equations to model a low-aspect, rectangular wing.(Preidikman and Mook,[4] in an earlier study of flutter of long-span suspension bridges, found limit-cycle responses when the structure was nonlinear.) Tang *et al.* used a crude version of the vortex-lattice method to predict the aerodynamic loads, calculating the loads on the undeformed flat plate even when there was deformation. We calculate the aerodynamic loads on the wing in its deformed position using a version of the vortex-lattice method that is inherently nonlinear and somewhat more refined than what Tang *et al.* used. Moreover, we include initial camber in the description of the wing. There are other significant differences between their approach and ours.

This article describes part of the work that was included in the first author's doctoral dissertation. More details, simulations of wind-excited oscillations of long-span bridges and the use of actively and passively controlled vanes attached to the bridges to suppress the wind-excited motions, and a rather extensive literature review can be found there.[5]

THE AERODYNAMIC MODEL

The boundary layers on the surfaces of the airplane are very thin regions of highly concentrated vorticity. The basic notion underlying the general unsteady vortex-lattice model is to imitate these boundary layers

as well as the wakes trailing from the aircraft as vortex sheets. We refer to these two types of vortex sheets as bound and free (wake) vortex sheets. Here we merge the upper and lower surfaces and place one bound vortex sheet on the camber surface of the wing. In Figure 1, we represent the free and bound vortex sheets used to model the wing of a modern business jet. In the figure, the wakes, which were calculated as part of the solution, are shown at various times steps following an impulsive start.

The circulations enclosing the elements of vortex lattice representing the wing, G_j, are determined by imposing the no-penetration condition. Using the Biot-Savart law, we express the velocity associated with the bound vortex sheet in terms of the circulations, obtain a set of linear algebraic equations, and solve for the circulations.

To generate the wake, we impose the Kutta condition by shedding vorticity from the trailing edge and wingtips. Then we convect the shed vorticity at the local particle velocity, using a system of first-order ordinary differential equations, keeping the circulations around the vortex segments in the wake constant, in order to render the wake force-free. Thus, vorticity in the wake now was generated on, and shed from, the wing earlier. As a result, the flow around, and the loads acting on the wing, now depend on what happened earlier; they are history-dependent and the "historian" is the wake.

The loads are calculated by multiplying the pressure difference across an element by the area of the element and the unit vector normal to the surface. Then the moments of these elemental forces are calculated. The time-varying pressure is calculated from the unsteady Bernoulli equation that has been modified to allow the evaluation of the time derivative of the potential at fixed point in the moving aerodynamic grid instead of at a fixed point in space.

THE STRUCTURAL MODEL

An airframe manufacturer generated the structural model of the wing using MSC/NASTRAN. They modeled the wing as a non-prismatic, linearly elastic, undamped, cantilevered beam with the root rigidly constrained. The bending and torsional stiffness distributions in the numerical model were adjusted so that the predicted free vibrations are in good agreement with the observations obtained in the ground vibration test. Simple two-node Euler-Bernoulli-beam (also known as cubic Hermitian) finite elements are used to model bending, and linear elements are used to model extension and torsion. In MSC/NASTRAN, torsion, bending around two axes, and extension are combined into a single element called "CBAR". The finite-element mesh used here has 28 nodes; they are on the elastic axis and each one has six degrees of freedom. Connected to the various structural nodes are rigid cross sections that have both rotary and translational inertia. The mass centers of these sections do not always fall on the elastic axes and they have rotary inertia; thus, there is dynamic coupling among torsion, extension, and bending.

The structural and aerodynamic grids are represented together in Figure 2. The structural nodes have six degrees of freedom and the aerodynamic nodes have three. We emphasize that the two grids can be arbitrarily selected. To describe the motion of the wing, we use an expansion in terms of the free-vibration modes of the beam. The time-dependent coefficients in this expansion are the generalized coordinates for the complete dynamic system.

In the next section we describe how the generalized structural forces are obtained from the aerodynamic loads, and how the generalized coordinates are used to obtain the motion of the aerodynamic grid.

COMBINING THE MODELS

We begin the description of how the structural and aerodynamic models are combined by relating the displacements of an arbitrary point, B, in the aerodynamic grid to the generalized structural nodal dis-

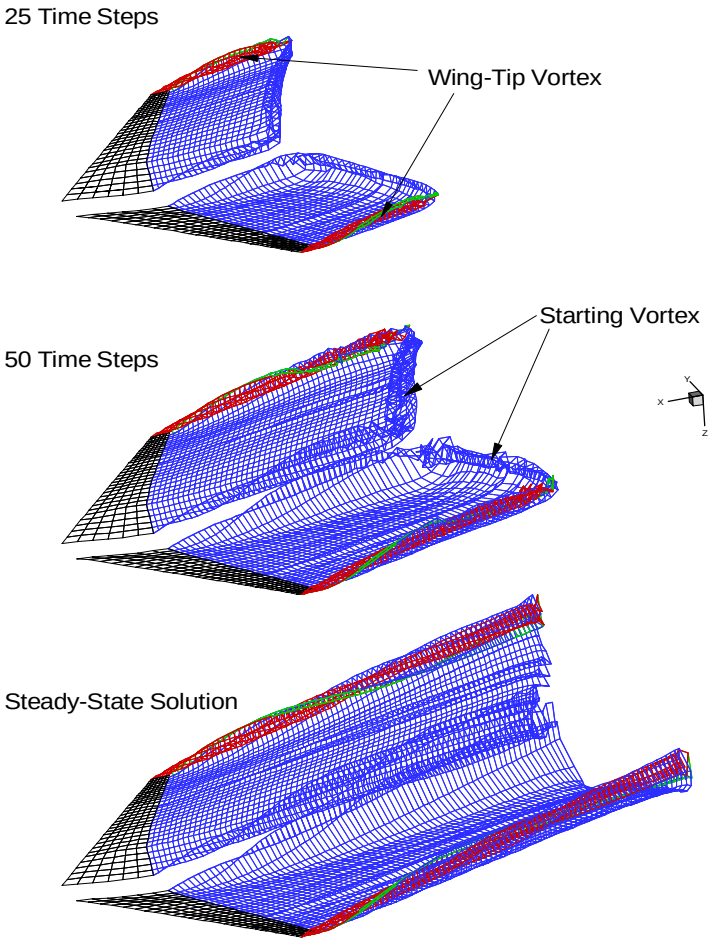

Figure 1: The solutions after 25 and 50 time steps, and the steady-state solution.

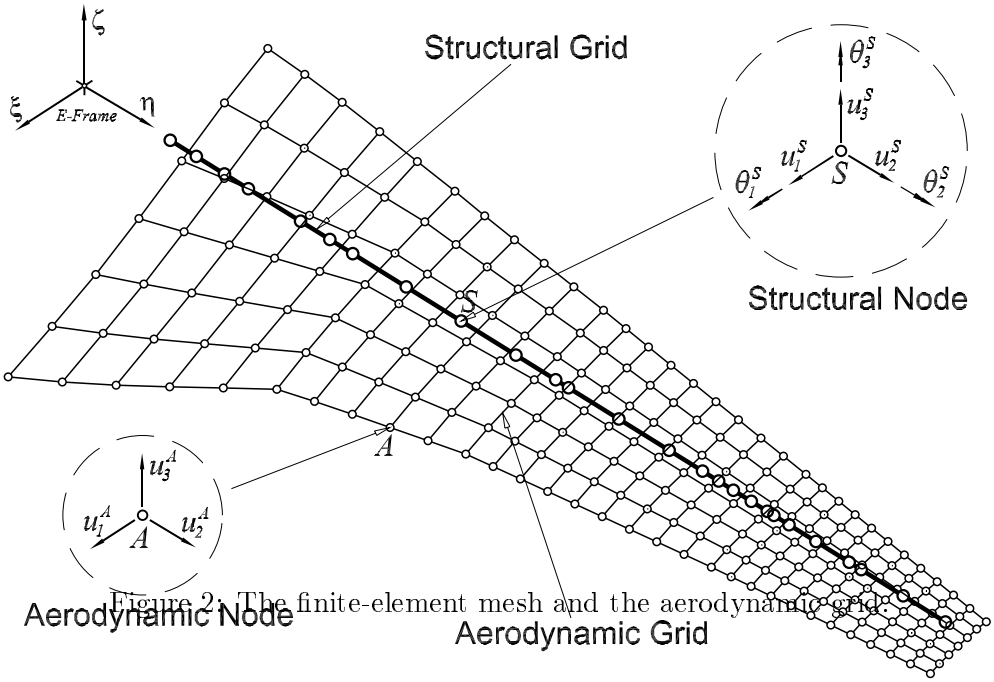

Figure 2: The finite-element mesh and the aerodynamic grid.

placements. After selecting point B, we find point A on the elastic axis such that points A and B lie in the same plane perpendicular to the elastic axis. In the elastic reference frame E, the coordinates of these points are (ξ_A, η_A, ζ_A) and (ξ_B, η_B, ζ_B). Both points have the same η-coordinate. We assume that sections perpendicular to the elastic axis are rigid and move and turn with the point on the axis where they are attached.

After the procedure is repeated for every selected point in the aerodynamic grid, we assemble a global matrix $\mathbf{G}_{AS}$ that maps the generalized displacements of all of the structural nodes into the displacements of all of the selected points in the aerodynamic grid. We use the same procedure to find the velocities of the control points in the aerodynamic grid where the boundary conditions are imposed on the flowfield.

To relate the structural forces $\mathbf{F}_S$ to the aerodynamic forces $\mathbf{F}_A$, we require the two force systems to do the same work for any virtual displacement.

INTEGRATING THE GOVERNING EQUATIONS

The numerical procedure is based on Hamming's fourth-order predictor-corrector method (see, *e.g.*, Carnahan *et al.*[6]). This scheme was chosen for two reasons: (1) the aerodynamic model provides better results when the loads are evaluated at only integral time steps, and (2) the aerodynamic loads contain contributions that are proportional to the acceleration. For both reasons Runge-Kutta type methods are not suitable, but predictor-corrector methods do not require the loads at fractions of the time step and, because they iterate, can treat acceleration on both sides of the equation. It turns out that the present numerical scheme, with some additional modifications, is also ideally suited for ship-dynamic problems (see, Preidikman *et al.*[7]).

There are two motions occurring simultaneously: both the wing and the wake are moving to the positions that they will occupy at the end of the next time step. And, as these movements are taking place, the distribution of vorticity on the wing is changing. We calculate the new positions of both the wing and the wake as well as the new distribution of vorticity on the wing simultaneously and interactively.

RESULTS

In this section we compute the unsteady aeroelastic response for a wing of the type that can be found on a modern business jet.

In Figure 3, the computed response to an initial disturbance is represented for two angles of attack; the seven modal(generalized) coordinates are plotted as functions of time. The speed is below the critical flutter speed, and all of the amplitudes decay to the steady-state values that correspond to the static deflection of the wing. The difference in the two responses is very noticeable; however, in both cases the third mode decays very slowly. This mode is the fore-and-aft, in-plane motion. There is no damping in the structural model, and the aerodynamic forces provide very little damping for this motion.

The response of the wing, which is a combination of all seven modes, clearly consists of components at many frequencies. At the lower angle of attack, there is considerable cross contamination of one mode by the others. At the higher angle of attack, the motion is a little more organized, with each mode having its energy somewhat concentrated around one frequency. Later we will see that as the flutter boundary is approached, the motion begins to organize, concentrating energy first around a few frequencies and finally around one. This result suggests that at a fixed speed it may be possible to induce flutter by increasing the angle of attack. In the next set of figures, we see how this organization evolves as the speed increases. The strengthening organization is a good indicator that the aircraft is nearing the flutter speed.

In Figure 4, the FFTs and histories are given for a series of responses at different speeds at the same angle of attack. Only the first (bending) and fourth (torsion) modes are shown in each plot. The wing has become

unstable between the last and next to last cases represented. In the last case, the frequencies of the two modes have clearly merged. In fact, all seven modes are now responding at the same frequency. Higher harmonics are apparent in the responses of the three highest modes, especially in that of the sixth mode. The motion of the third mode contains its strongest component at the merged torsion-bending frequency; that is, the in-plane motion is now also responding at the merged frequency, but there is some energy at a higher frequency, which also appears to be a harmonic of the merged frequency. The transitions from the natural frequencies of the modes to the common frequency of flutter are also apparent in these plots, especially in the one for the second mode.

Unstable (after the onset of flutter) responses are represented in Figure 5. They are limit cycles. The growth in the steady-state amplitudes of the limit cycles as a function of speed is not explosive, but appears to start at zero; therefore, the instability is most likely a supercritical Hopf bifurcation. It is questionable whether the first two responses should be considered unstable. They are near the critical and perhaps would decay completely if the solution were extended for more time. The amplitudes of the remaining responses grow linearly with time, at least initially, as one would expect from the classical analysis of flutter. For these responses to be true limit cycles, the motion must evolve into the same steady-state response for all initial conditions. We have found that such is the case. The motion is dominated by the first, third, and fourth modes. As expected, for the reasons mentioned above, the response in the third mode contains more than one frequency.

Returning to Figure 5, we note that, as the speed continues to increase above the flutter speed, the amplitude of the limit cycle continues to grow and eventually begins to modulate, slightly at first and then quite noticeably. This behavior, which is first noticeable in the third-from-last response represented in the figure, indicates that the motion has passed through a second super-critical Hopf bifurcation, and that the amplitude and frequency of the response modulate. The response in this case is often described as motion on a torus. The FFT of the first mode shows side bands and extra frequency associated with motion on a torus. The nonlinear behavior that appears here is solely the result of having a nonlinear aerodynamic model; the structural model is linear. Also, computer movies of the modulated responses show rather large deformations, especially in torsion, and suggest that the structure will break before such behavior develops in a real aircraft. Finally, we emphasize that all of the instabilities found in the present simulations occurred well outside the flight envelope of the aircraft used in the numerical example.

CONCLUDING REMARKS

A method for simulating the unsteady aeroelastic behavior of wings has been developed. The flowing air and the deforming wing structure are treated as elements of the same dynamic system. The present development is consistent with such industry-standard programs as CATIA and MSC/NASTRAN. The simulation consists of four parts: an aerodynamic model to predict the load on the wing, a structural model to predict the response of the wing to this load and to provide the boundary conditions on the flowfield, a scheme for the two models to communicate with each other, and a method to integrate the governing equations of the complete system. The deformation of the wing is expressed as an expansion in terms of its linear free-vibration modes, which are determined from the structural model. The time-dependent coefficients in this expansion are the generalized coordinates for the entire dynamic system, and the equations governing them are integrated numerically in the time domain. The simulation is organized in modules so that the aerodynamic and structural models can be changed without changing the basic organization of the simulation.

As a numerical example to illustrate the method, we studied the response of a wing which is representative of that of a modern business jet. The numerical results predict that at low speeds all initial disturbances decay; that as the speed increases, the organization of the response becomes more organized; and that eventually the frequencies in the response merge into a single frequency. Coincident with the merger of frequencies, the response becomes unstable. In the initial portion of an unstable response, the amplitude of

the motion grows linearly with time; subsequently the response develops into a limit cycle. The amplitudes of the limit cycles are rather small initially, but grow as the speed increases; this is behavior which suggests that the bifurcation is supercritical. If the speed increases sufficiently, the response appears to experience a secondary, supercritical Hopf bifurcation after which the amplitude and the phase of the response modulate. At this point the response can be described as motion on a torus.

The rich nonlinear behavior of this dynamic system is due entirely to the aerodynamic model, which is inherently nonlinear. Earlier studies found limit cycles in the response when nonlinear structural models were used. Here the structural model is linear and the aerodynamic model is nonlinear. When nonlinear structural models are used in future simulations, we expect to see an even greater range of nonlinear phenomena.

REFERENCES

[1] T. W. Strganac and D. Mook, "A numerical model of subsonic aeroelastic behavior," *AIAA Journal* **28**, pp. 903–906, 1990.

[2] J. Luton and D. Mook, "Numerical simulations of flutter and its suppression by active control," *AIAA Journal* **31**(12), pp. 2312–2319, 1993.

[3] D. Tang, E. Dowell, and K. Hall, "Limit cycle oscillations of a cantilevered wing in low subsonic flow," *AIAA Journal* **37**(3), pp. 364–371, 1999.

[4] S. Preidikman and D. Mook, "Numerical simulation of flutter of suspension bridges," *Applied Mechanics Reviews* **50**, pp. 174–179, 1997.

[5] S. Preidikman, *Numerical Simulations of Interactions Among Aerodynamics, Structural Dynamics, and Control Systems*. PhD thesis, Virginia Polytechnic Institute and State University, 1998.

[6] B. Carnahan, H. Luther, and J. Wilkes, *Applied Numerical Methods*, Wiley, New York, 1969.

[7] S. Preidikman, D. Mook, and A. Nayfeh, "On modifying hamming's method to treat fluid/body interactions," in *PACAM VI/DYNAME 99*, (Rio de Janeiro, Brazil), January 4–8 1999.

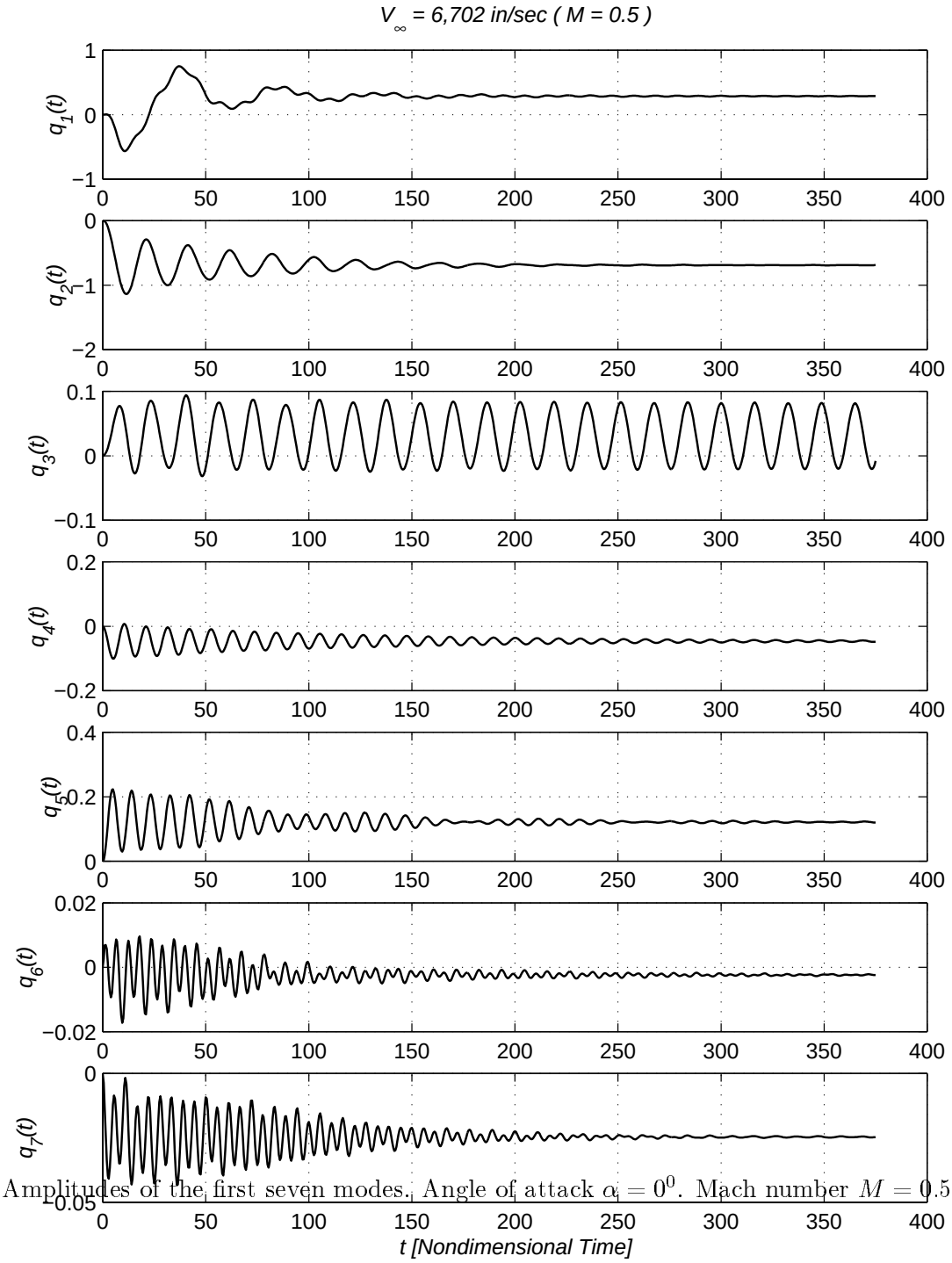

Figure 3: Amplitudes of the first seven modes. Angle of attack $\alpha = 0^0$. Mach number $M = 0.5$. Sea level.

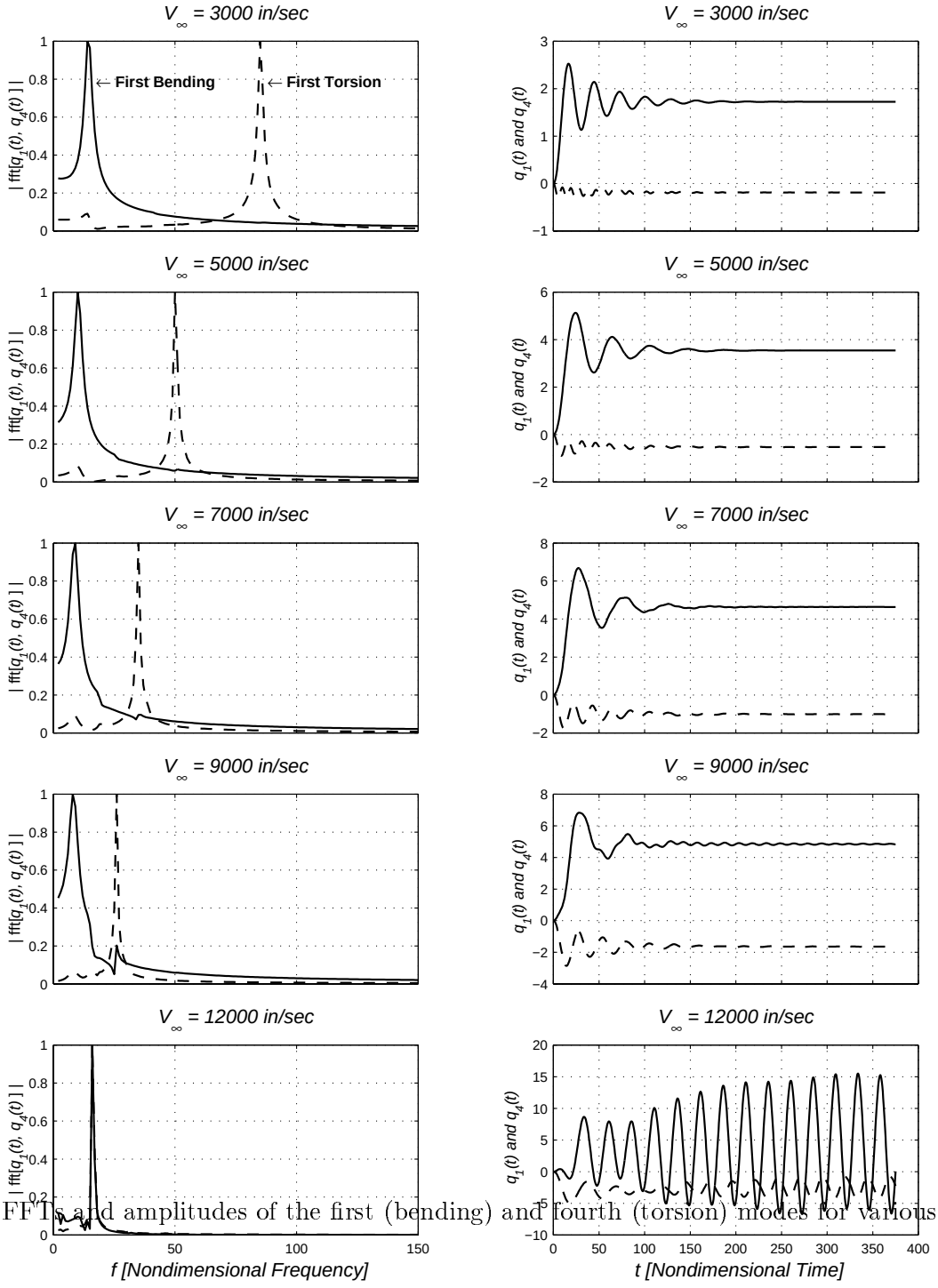

Figure 4: FFTs and amplitudes of the first (bending) and fourth (torsion) modes for various airspeeds.

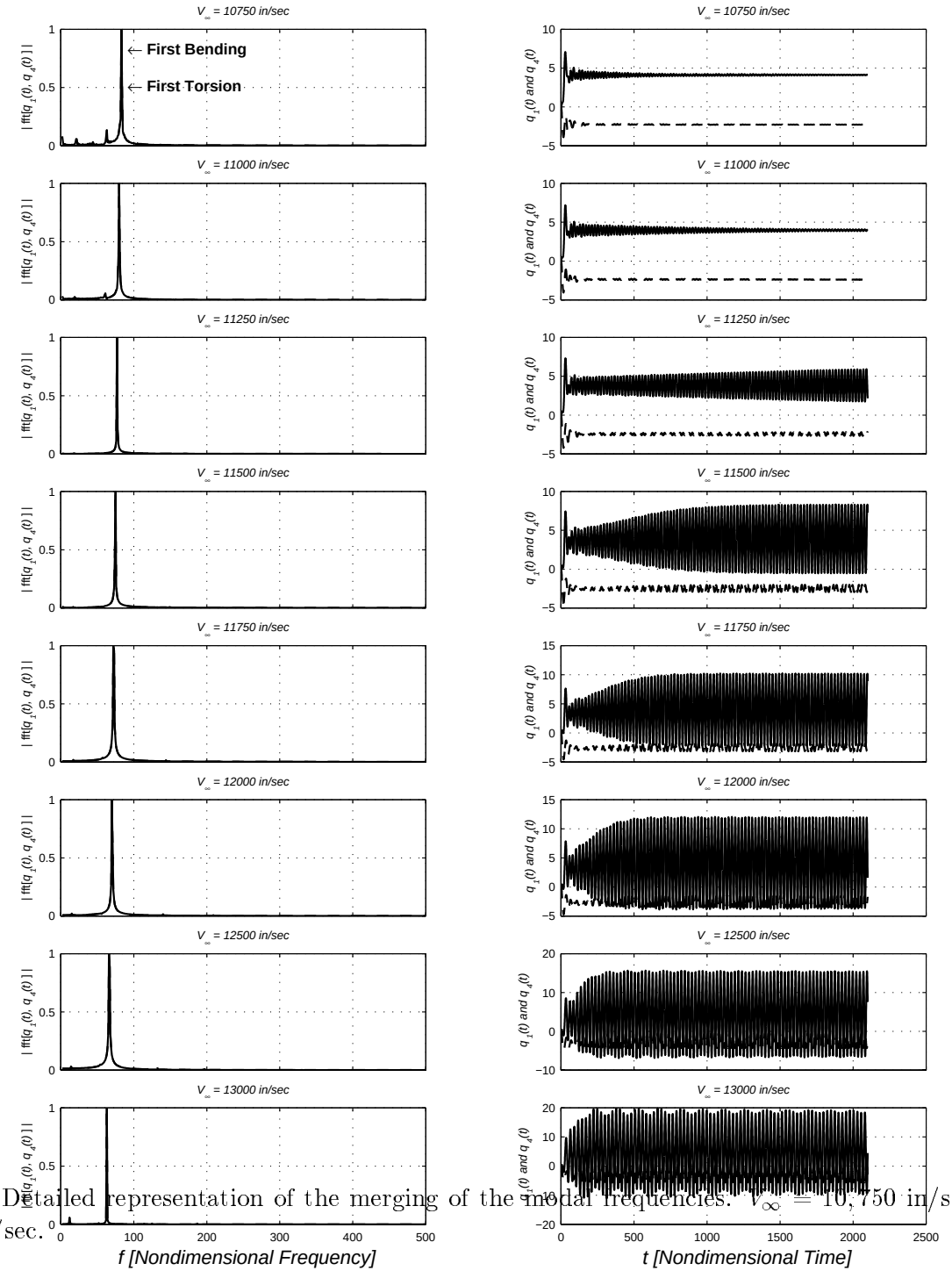

Figure 5: Detailed representation of the merging of the modal frequencies. $V_\infty = 10,750$ in/sec to $V_\infty = 13,000$ in/sec.